HHS Public Access

Author manuscript

Anat Rec (Hoboken). Author manuscript; available in PMC 2021 June 01.

Published in final edited form as:

Anat Rec (Hoboken). 2020 June ; 303(6): 1630–1641. doi:10.1002/ar.24109.

Neuronal PAS Domain 2 (*Npas2*)-Deficient Fibroblasts Accelerate Skin Wound Healing and Dermal Collagen Reconstruction

HODAKA SASAKI[1,2], **AKISHIGE HOKUGO**[1,3], **LIXIN WANG**[1,3], **KENZO MORINAGA**[1,4], **JOHN T. NGO**[1], **HIROKO OKAWA**[1,5], **ICHIRO NISHIMURA**[1,*]

[1]Weintraub Center for Reconstructive Biotechnology, UCLA School of Dentistry, Los Angeles, California

[2]Department of Oral and Maxillofacial Implantology, Tokyo Dental College, Tokyo, Japan

[3]Regenerative Bioengineering and Repair Laboratory, Division of Plastic and Reconstructive Surgery, Department of Surgery, David Geffen School of Medicine at UCLA, Los Angeles, California

[4]Department of Oral Rehabilitation, Section of Oral Implantology, Fukuoka Dental College, Fukuoka, Japan

[5]Division of Molecular and Regenerative Prosthodontics, Tohoku University Graduate School of Dentistry, Sendai, Japan

Abstract

The circadian clock, which consists of endogenous self-sustained and cell-autonomous oscillations in mammalian cells, is known to regulate a wide range of peripheral tissues. The unique upregulation of a clock gene, neuronal PAS domain protein 2 (*Npas2*), observed along with fibroblast aging prompted us to investigate the role of *Npas2* in the homeostasis of dermal structure using in vivo and in vitro wound healing models. Time-course healing of a full-thickness skin punched wound exhibited significantly faster wound closure in *Npas2*−/− mice than wild-type (WT) C57Bl/6J mice. Dorsal skin fibroblasts isolated from WT, *Npas2*+/−, and *Npas2*−/− mice exhibited consistent profiles of core clock gene expression except for *Npas2* and *Per2*. *In vitro* behavioral characterizations of dermal fibroblasts revealed that *Npas2*−/− mutation was associated with increased proliferation, migration, and cell contraction measured by floating collagen gel contraction and single-cell force contraction assays. *Npas2* knockout fibroblasts carrying sustained the high expression level of type XII and XIV FAICT collagens and synthesized dermis-like thick collagen fibers *in vitro*. Confocal laser scanning microscopy demonstrated the reconstruction of dermis-like collagen architecture in the wound healing area of *Npas2*−/− mice. This study indicates that the induced *Npas2* expression in fibroblasts may interfere with skin homeostasis, wound healing, and dermal tissue reconstruction, providing a basis for novel therapeutic target and strategy.

*Correspondence to: Ichiro Nishimura, Weintraub Center for Reconstructive Biotechnology, UCLA School of Dentistry, Box 951668, CHS B3-087, Los Angeles, CA 90095. Tel: +1 (310) 794-7612, Fax: +1 (310) 825-6345, inishimura@dentistry.ucla.edu.

This article includes AR WOW Video. Video can be viewed at https://players.brightcove.net/656326989001/default_default/index.html?videoId=6013197672001.

Keywords

Npas2; fibroblast; wound healing; collagen; circadian rhythm

INTRODUCTION

The circadian rhythm, known as endogenous self-sustained and cell-autonomous oscillations of 24 hr rhythms in mammalian cells, is responsible for a wide range of physiological homeostasis functions (Franzoni et al., 2017), and the disruption of this rhythm is involved in chronic diseases, such as cardiovascular disease, diabetes, metabolic and sleep disorders, infertility, and impaired wound healing (Miller et al., 2004; Turek et al., 2005; Oishi et al., 2006; Wijnen and Young, 2006; O'Neil et al., 2013; Sipahi et al., 2014). A previous study reported that the database of human burn injuries showed that wounds injured during the night (the rest period) healed more slowly than wounds acquired during the day (the active period) (Hoyle et al., 2017). Those results suggest a regulatory role of circadian rhythm in wound healing, albeit the mechanism of how the circadian rhythm contributes to skin wound healing is still unclear.

Circadian rhythm is regulated in the central brain by the suprachiasmatic nuclei (SCN) of the hypothalamus, which is the circadian pacemaker (Akhtar et al., 2002; O'Neil et al., 2013). One of the circadian rhythm core regulators, neuronal PAS domain protein2 (NPAS2) is a member of the basic helix-loop-helix (bHLH)-PAS family of transcription factors and is a paralog of the circadian locomotor output cycles kaput (CLOCK). NPAS2 or CLOCK dimerizes with brain and muscle Arnt-like protein-1 (BMAL1) to regulate the gene transcription of two other circadian gene clusters; period (PER) and cryptochrome (CRY). PER and CRY then suppress the expression of NAPS2, CLOCK, and BMAL1 by a transcription/translation feedback loop system (Vitaterna et al., 1994; Bunger et al., 2000). Previous studies have revealed that *Npas2* expression occurs in the mammalian forebrain and central brain but not in the SCN. However, the distinct expression of *Npas2* was reported in peripheral tissue, including the heart, liver, vasculature, and skin (Zhou et al., 1997; McNamara et al., 2001; Gilles-Gonzalez and Gonzalez, 2004; Yamamoto et al., 2004; Bertolucci et al., 2008).

Mouse skin fibroblasts have been reported to express *Npas2,* which might compensate for the lack of *Clock* expression (Landgraf et al., 2016). *NPAS2* was identified among significantly upregulated genes in aging human skin by microarray analysis (Glass et al., 2013). Taken together, we have hypothesized that *Npas2* in skin fibroblasts plays a key role in homeostatic maintenance, and therefore is a key factor during skin wound healing. The objective of our study was to address this hypothesis using *Npas2* knockout mice.

MATERIALS AND METHODS

Animal Ethics Statement

The *Npas2* knockout (KO) mice (B6.129S6-Npas2tm1Slm/ J,Jackson Laboratory, Bar Harbor, ME) of the c57B1/6J background were used in this experiment. *Npas2* heterozygous

mutant *(Npas2+/−)* mice were generated from cryopreserved sperm samples, and an active breeding colony was established at UCLA. Both *Npas2*−/− and *Npas2*+/− mice were used as the experimental groups, and C57Bl/6J wild-type (WT) mice were used as the control group. All of the experimental protocols using animals were reviewed and approved by the UCLA animal research committee (ARC# 2003–009) and followed the Public Health Service Policy for the Humane Care and Use of Laboratory Animals and the UCLA Animal Care and Use Training Manual guidelines. All of the animals had free access to food and water and were maintained in regular housing with a 12 hr light/dark cycle at the Division of Laboratory Animal Medicine, UCLA.

Mouse Dorsal Skin Full-Thickness Excisional Wound Model

The 9- to 14-week-old mice weighing approximately 25 g (WT: four males and four females, Npas2+/−: seven males and Npas2 −/−: seven males) were used for the dorsal skin full-thickness wound experiment. After anesthesia with isoflurane inhalation, identical skin wounds were created on the right and left sides of dorsal skin simultaneously by punching a full-thickness skin wound, passing though the *panniculus carnosus* layer, with a 5 mm dermal biopsy punch (INTEGRA, Integra Life Sciences, Plainsboro, Nj). These surgeries were performed between 11 a.m. and 1 p. m. Standardized photographs during the course of wound healing were obtained at 0, 2, 4, 6, and 12 days. The skin wound area was measured at each time point (NIH ImageJ ver.1.51). The wound areas on each day were compared by the Kruskal-Wallis test with Dunn's post-test. These mice were sacrificed at 7 days (n = 4 in each group) and 14 days (WT: four mice, Npas2+/−: three mice, and Npas2−/−: three mice) for histological analysis. The dorsal skin containing the wound area was dissected as a 1 cm square and immediately fixed with 10% neutral buffered formalin. The sections were stained with hematoxylin and eosin (H-E) for histological evaluation.

Dermal Fibroblast Cell Culture

Primary fibroblasts from the mouse dorsal skin of each of the three genotypes were cultured using an explant method. The cells were cultured in Dulbecco's modified Eagle's medium (DMEM) with 10% fetal bovine serum and 100 U penicillin/0.1 mg/mL streptomycin at 37°C, 5% CO2 in a humidified incubator. Their genotype was determined by polymerase chain reaction (PCR) targeting WT and mutant *Npas2* gene alleles.

WST-1 Cell Proliferation Assay

The cell proliferation assay was performed using WST-1 reagent (Roche Applied Science, Indianapolis, IN). A total of 2,000 cells were seeded into a 96-well reading plate and cultured for the predetermined time points (Days 1, 3, 5, and 7). At each time point, the culture medium was changed to 10% WST-1 regent with medium and incubated for 3 hr (n = 4 per time point). The absorption value was read in a spectrophotometer at 450 nm with a plate reader (SYHNERGY H1 plate reader, Biotek, Winooski, VT) and compared by two-way analysis of variance (ANOVA), followed by the Tukey test at each time point.

Circadian Gene Expression in Skin Fibroblasts

Steady-state mRNA expression levels of eight core circadian genes in skin fibroblasts were determined by quantitative real-time PCR (RT-PCR) using Taqman MGB probes (Thermo Fisher Scientific Inc., Waltham, MA). Fibroblasts were cultured in 24-well plates and synchronized at 80% to 90% confluency by adding 100 nM dexa- methasone to the medium and incubating for 2 hr, followed by washing with DMEM (Nagoshi et al., 2004). Total RNA was extracted using an RNeasy kit (Qiagen, Valencia, CA) every 6 hr, starting at 0 −48 hr (n = 4 per time point) after the synchronization, and their quality and quantity were confirmed by NanoDrop (Thermo Fisher Scientific Inc.). The RT-PCR was performed using commercially available primer/probe mixes (Thermo Fisher Scientific Inc.) as follows: *Npas2* (Mm01239312_m1), *Bmal1* (= Arntl: Mm00500223_m1), *Clock* (Mm00455950_m1), *Per1* (Mm0050 1813_m1), *Per2* (Mm00478099_m1), *Per3* (Mm00478120_m1), *Cry1* (Mm00514392_m1), and *Cry2* (Mm01331539_m1). *Gapdh* was used as an internal control. In addition, the *LacZ* reporter gene expression was determined. The statistical analysis was performed first by two-way ANOVA. The group with the significant interaction P value ($P < 0.05$) by two-way ANOVA and the gene expression at each time point was further subjected to the Tukey test.

In Vitro Wound Healing Scratch Plate Assay

Fibroblasts were seeded into a 6-well plate and were synchronized as above. After 2 hr, scratch lines were created with a 20 μL plastic pipette and were washed with medium (n = 5 per group). These scratched areas were captured by time-lapse photomicrography every hour from 0 to 24 hr. The number of migrated cells into the scratched area was counted at 12 and 24 hr and compared by one-way ANOVA with *post hoc* Holm test.

Floating Collagen Gel Contraction Assay

The floating collagen gel contraction assay was performed following the previously established protocol with some modifications (Ngo et al., 2006). A 500 μL aliquot of collagen gel mixture (Collagen Type I, Corning, Manassas, VA) containing fibroblasts (50,000 cells) was applied to a 24-well plate (n = 5 in each group) and placed at room temperature for 20 min. The solidified gels were transferred to a 100 mm diameter dish and cultured (37°C, 5% CO_2 in a humidified incubator). The gel images were scanned by a scanner at 0, 6, 12, 24, 48, and 72 hr. The collagen gel area at each time point was measured (NIH ImageJ ver.1.51) and compared by two-way ANOVA, followed by the Tukey test at each time point.

Single-Cell Contraction Assessment

Single-cell contraction was measured using fluorescently labeled elastomeric contractible surfaces (FLECS) (Forcyte Biotechnologies Inc., Los Angeles, CA) (Koziol-White et al., 2016). FLECS plates with the soft silicone elastomer filmed bottom were micropatterned with fluorescent fibrinogen in uniform “X” shapes (70 μm diagonal by 10 μm thick). Approximately 30,000 cells were seeded into a well of 24-well

FLECS plate. The plates were placed at room temperature for 40 min and in an incubator (37°C, 5% CO_2) for 30 min for cell attachment. After incubation for initial cell attachment

to the X-shape pattern, floating cells were removed by washing with medium, and the plates were incubated for an additional 8 hr. Nuclear staining was performed with Hoechst 33,342 (1:10,000). The images of the fluorescent fibrinogen on the X-shape patterns were captured using a fluorescence microscope with a rhodamine filter. For single-cell contraction evaluation, micropatterns associated with a single nucleus attached at the center of the X shape were selected and categorized to either the no-contract or contract group by comparison with the no-cell pattern. The ratio of contracted patterns per captured image (containing approximately 1,000 X-shape patterns) was compared among each genotype (n = 5). The statistical analysis was performed by one-way ANOVA with the *post hoc* Holm test.

Gene Expression for Actin, Integrin, and Collagen Subunits

Total RNA samples were extracted from fibroblasts every 6 hr, from 24 to 48 hr after synchronization, as described above. The RNA samples were used for evaluating the gene expression of actin subunits —β-actin (*Actb*: Mm02619580_g1) and α-smooth muscle actin (α-SMA, *Acta2:* Mm00725412_s1) (Fig. 3G); integrin subunits—integrin αV (*ItgaV:* Mm00434486_m1), integrin β3 (*Itgb3:* Mm00443980_m1), and integrin β5 *(Itgb5:* Mm00439825_m1) (Fig. 3H); and collagen subunits—type I *(Col1a1:* Mm00801666_g1 and *Col1a2:* Mm00483888_m1), type III *(Col3a1:* Mm00802300_m1), type XII *(Col12a1:* Mm01148576_m1) and type XIV *(Col14a1:* Mm008052 69_m1) by Taqman-based qRT-PCR (Fig. 4A). The statistical analysis was performed by two-way ANOVA and Tukey test at each time point.

Collagen Synthesis Assessment in vitro by Picrosirius Red Staining

Fibroblasts were seeded into 24-well plates and cultured at 80%−90% confluency in medium supplemented with ascorbic acid (50 μg/mL) for 1, 3, and 7 days. The cells were then fixed with 10% neutral buffered formalin and stained with picrosirius red (PolyScience, Niles, IL) for visualizing the collagen. The absorption value was read in a spectrophotometer at 550 nm with a plate reader (SYHNERGY H1 plate reader) and compared by one-way ANOVA with the *post hoc* Holm test.

Collagen Fiber Structure at Skin Wound Healing Area by Picrosirius Red Staining and Confocal Laser Scanning Microscopy

The histological sections for the dorsal skin full-thickness wound experiment at 7 and 14 days after surgery were stained with picrosirius red for collagen fibers during wound healing. Collagen fiber structure in the granulation tissue (GT) area, wound closure area (WCA), and intact skin area (ISA) was evaluated using confocal laser scanning microscopy. The distance between the edge of the *panniculus car- nosus* as the original wound width (a) and the distance between the edge of the maturated collagen at the skin punch area, measured as the width of GT (b), were assessed. The ratio of wound closure was calculated by (a - b)/a and was compared by the Kruskal-Wallis test with Dunn's *post hoc* test.

RESULTS

Full-Thickness Dorsal Skin Wound Closure Was Accelerated in Npas2–/– Mice

The full-thickness dorsal skin wounds contracted continuously from Days 2 to 12 after surgery, and scar formation was recognized by Day 12 in all genotypes (Fig. 1A). The relative wound area at Day 12 in Npas2−/− mice was significantly smaller than in the other two genotypes ($P < 0.01$) (Fig. 1B). In the histological observation, hyperkeratosis, residual clots, and the immune response in the GT area were observed at 7 days after surgery. Furthermore, the edge of dermis connective tissue with hair follicles moved toward the center of wounds by Day 14. The epithelial layer at the wound area appeared to be similar to the intact skin epithelium, and the immune response had declined in all samples (Fig. 1C). In the present study, mouse dorsal skin full-thickness excisional wounds were generated in the middle of the day (11 a.m.−1 p.m.). It has been reported that skin burn wounds occurring during the night or resting period of humans showed impaired healing (Hoyle et al., 2017). Daytime for the nocturnal mice is equivalent to night for humans. It may be possible that the difference in wound healing between WT and Npas2 KO mice might be more evident if the wound occurred during the dark/active period in mice.

The Effect of Npas2 KO Mutation on Proliferation and Circadian Rhythm Gene Expression of Skin Fibroblasts

The genotype for each fibroblast sample was determined by PCR. Exon 2 of the mouse *Npas2* allele was replaced by the *LacZ* expression reporter cassette (LacZ/Neo). Because exon 2 encodes the bHLH sequence, the resultant Npas2 molecule lacked the DNA binding function. The amplified PCR product, which was larger than that of WT, recognized *Npas2*−/− fibroblasts and both the mutant and WT PCR products recognized Npas2+/− fibroblasts.

The WST-1 assay indicated that both *Npas2*+/− and *Npas2*−/− fibroblasts proliferated faster than WT fibroblasts ($P < 0.01$) (Fig. 2b).

The circadian expression of *Npas2* was decreased in *Npas2*+/− fibroblasts and was undetected in *Npas2*−/− fibroblasts. However, an effect of the *Npas2* KO mutation on the expression patterns of other circadian genes was not observed, except for the *Per2* expression (Fig. 2C). The reporter gene (*LacZ* expression) was detected only in *Npas2* KO mice.

Accelerated in vitro Wound Healing of Npas2–/– Skin Fibroblasts by Scratch Test and Floating Collagen Gel Contraction Assay

The wound healing scratch assay, floating collagen gel contraction assay, and single-cell force assessment with FLECS were performed *in vitro.* The numbers of migrated *Npas2*+/− and *Npas2*−/− fibroblasts were higher than those of WT during 24 hr (Video: https://players.brightcove.net/656326989001/default_default/index.html?videoId=6013197672001), which was statistically significant ($P < 0.05$) (Fig. 3A,B). However, there was no significant difference between the cell migration rate of *Npas2*+/− and *Npas2*−/− fibroblasts (Fig.

3A,B). The floating collagen gel contraction assay showed that *Npas2*−/− fibroblasts contracted faster than WT and *Npas2*+/− fibroblasts ($P < 0.01$) (Fig. 3C,D).

Single-Cell Contraction and Expression of α-SMA and Integrins

The evaluation for single-cell contraction using FLECS (Fig. 3E) revealed that the ratio of contracted *Npas2*+/− and *Npas2*−/− fibroblasts was higher than the ratio of WT fibroblasts ($P < 0.01$) (Fig. 3F). The gene expression levels of β-actin *(Actb),* known to be related with cell migration, and α-SMA (*Acta2*), known as the factor for upregulating myofibroblast contractile activity, were evaluated by RT-PCR (Fig. 3G). The expression of both actin subunits decreased over time. However, there was no significant difference among the three genotypes. The expression of integrin αV (*ItgaV*), integrin β3 (*Itgb3*), and integrin β5 (*Itgb5*) did not show any circadian rhythm in dermal fibroblasts. Npas2 KO mutation did not affect the steady-state level of the examined integrin subunits (Fig. 3H).

Npas2–/– Fibroblasts Increased Dermis-Like Collagen Synthesis In Vitro

The gene expression levels of collagen subunits type I (*Col1a1, Col1a2*), type III (*Col3a1*), type XII (*Col12a1*), and type XIV (*Col14a1*) were investigated in this experiment (Fig. 4A). Overall, no circadian pattern was observed in these collagen mRNAs. *Col1a1* and *Col1a2* in *Npas2*−/− fibroblast were more highly expressed than in WT and Npas2+/− fibroblasts; however, the interaction *P* value was significant only for *Col1a2.* No difference was observed for the *Col3a1* expression. There was an increase of *Col12a1* expression in *Npas2*+/− and *Npas2*−/− fibroblasts. Strikingly, a significantly elevated expression of *Col14a1* was found in both *Npas2*+/− and *Npas2*−/− fibroblasts compared to WT fibroblasts. The picrosirius red staining for fibroblasts cultured with ascorbic acid supplementation showed a strong, positive reaction, indicating collagen fiber formation and accumulation in *Npas2*+/− and *Npas2*−/− fibroblasts (Fig. 4B); their absorbance at 550 nm was significantly higher than that in WT fibroblasts at Day 7 ($P < 0.01$) (Fig. 4C).

Dermis-Like Collagen Fiber Reconstruction during Skin Wound Healing of Npas2–/– Mice

Histological sections of the full-thickness skin wound area with picrosirius red staining were examined by con-focal laser scanning microscopy (Fig. 5A). There was no obvious difference in collagen fiber structures in the ISA; however, collagen fibers in both the GT area and the WCA appeared to be thicker in *Npas2*+/− and *Npas2*−/− samples than in those of WT. In particular, collagen fibers of GT in *Npas2*−/− samples appeared more organized, partially resembling the intact skin collagen structure. The histological measurement of wound closure was performed with picrosirius red-stained sections (Fig. 5B). The ratio of wound closure of *Npas2*+/− and *Npas2*−/− samples was greater than that of WT, although statistical significance was achieved only between WT and *Npas2* −/− samples at Day 14 ($P < 0.01$) (Fig. 5C).

DISCUSSION

Mammalian skin is a large barrier tissue composed of the epithelial layer (epidermis) and underlining connective tissue (dermis). This study proposes a novel role of the circadian clock in dermal fibroblasts for skin wound healing, which may possibly enable dermal

connective tissue collagen reconstruction. Once injured, the skin epithelial cells actively proliferate and migrate over the wound, leading to the rapid establishment of a barrier layer. By contrast, dermal fibroblasts are slow in proliferation and migration into the wound area. Furthermore, wound fibroblasts do not maintain the dermal fibroblast phenotype, but acquire a new phenotype, in part, contributing to the formation of GT and scarring. The present study demonstrated the accelerated healing of the well- established skin full-thickness wound model (Kowalska et al., 2013) in Npas2 $^{+/-}$ and Npas2 $^{-/-}$ mice, potentially through faster wound closure and/or smaller scarring than that of WT mice (Fig. 1). As such, this study focused on the role of Npas2 KO mutation on the behavior of dermal fibroblasts as a mechanistic investigation.

Npas2 is a core circadian rhythm gene encoding a basic HLH transcription factor and is highly expressed in skin fibroblasts. *Npas2* has been postulated to compensate the role of *Clock,* whose expression rate in fibroblasts was comparatively low (Fig. 2C) (Landgraf et al., 2016). In the case of retinal cells, knock down of the *Clock* gene reduced mRNA and protein levels of *Npas2*, whereas knock down of *Npas2* did not affect either the mRNA or protein levels of *Clock* (Haque et al., 2010). Our data corroborated the previous observation that *Npas2* KO mutation did not significantly affect the expression of the core circadian rhythm genes (Fig. 2C). Thus, the effect of *Npas2* KO mutation may be mediated by mechanisms other than the disruption of the circadian rhythm. The expression of *Npas2* in the SCN peaks at the dark/active period in mice (Haque et al., 2010). Wound responses in mice would be expected to show a daily rhythm. However, we did not explore this issue in the present study.

Three-dimensional collagen gels containing fibroblasts have been used to model tissue remodeling, wound contraction, and fibrosis (Grinnell, 1994). The primary mechanism of fibroblast-embedded gel contraction *in vitro* is due to fibroblast locomotion forces (Ehrlich and Rajaratnam, 1990). The cell traction force is applied to the substrate ECM, contributing to the collagen gel contraction (Brown et al., 2002). The accelerated collagen gel contraction was demonstrated by *Npas2*$^{+/-}$ and *Npas2*$^{-/-}$ fibroblasts (Fig. 3C,D), suggesting the increased fibroblast locomotion forces. It was reported that silencing the *NPAS2* expression in human colorectal cancer cells accelerated cell migration (Xue et al., 2014). The present study also showed accelerated migration by *Npas2*$^{+/-}$ and *Npas2*$^{-/-}$ fibroblasts in an *in vitro* scratch test (Video: https://players.brightcove.net/656326989001/default_default/index.html?videoId=6013197672001; Fig. 3A,B). The activation of extracellular signal-regulated kinase (ERK) and phosphoinositide-3 kinase/protein kinase B (PI3K/AKT) through phosphorylation is well known to regulate cell migration, collagen gel contraction, and skin wound healing (Liu et al., 2008; Chen et al., 2014; Li et al., 2016). The activation of these signaling pathways was suggested in the phenotype conversion of fibroblasts toward myofibroblasts, such as an increased expression of α-SMA (Mulero-Navarro et al., 2005). In our study, the phenotype conversion of fibroblasts was not suggested by the *Npas2* KO mutation (Fig. 3G), and thus, the involvement of a myofibroblast-like phenotype in the modulated collagen gel contraction and fibroblast migration was ruled out. However, it is important to characterize the effect of *Npas2* KO mutation on phosphorylation in the ERK/Akt/FAK pathway.

During migration, fibroblasts adhere to the extracellular matrix (ECM) through integrin molecules and generate a single-cell traction force (Style et al., 2014). We used a recently developed single-cell contraction assay that required cell adhesion to the FLECS printed with fibronectin (Koziol-White et al., 2016; Pushkarsky et al., 2018). The FLECS assay showed that mouse dermal fibroblasts increased the cell contraction behavior by *Npas2* KO mutation (Fig. 3F). Wound-induced transformation of fibroblasts to myofibroblasts has been postulated to play a pathological role in tissue contraction and fibrosis formation (Kendall and Feghali-Bostwick, 2014). Separately, the increased expression of alpha and beta integrins mediating cell adhesion to fibronectin were thought to be critical for cell contractility-driven wound fibrosis formation (Conroy et al., 2016). For example, the significantly elevated expression of integrin αVβ3 has been postulated to cause idiopathic pulmonary fibrosis (Fiore et al., 2018). In the present study, the steady-state expression of myofibroblast marker α-SMA as well as integrin subunits αV, β3, and β5 was not altered by *Npas2* KO mutation in dermal fibroblasts (Fig. 3G,H). Therefore, the increased fibroblast contractility by *Npas2* KO mutation may not result in the abnormal wound healing phenotypes of pathological wound contraction or fibrosis formation.

Connective tissue ECM molecules, in particular the FACIT class of collagens, have been shown to influence cell migration and cell contraction through integrin-mediated cell adhesion (Schiro et al., 1991; Nishiyama et al., 1994; Grässel and Bauer, 2013). The FACIT class of collagens has been postulated to decorate the surface of collagen fibers (Klein et al., 1998). The externally exposed N-terminal globular domains, such as NC3 of type XII and type XIV colla-gens, have been shown to be essential in fibroblast-mediated collagen gel contraction (Nishiyama et al, 1994). Thus, we postulate that the increased expression of type XII and XIV collagens in Npas2 KO fibroblasts might affect the migration and gel contraction behaviors.

It has been reported that downregulation of *Npas2* expression is related to cell cycle progression and DNA repair capacity (Zhu et al., 2007; Zhu et al., 2008), although there are conflicting reports on the effect of *Npas2* modulation on cell proliferation (Xue et al., 2014; Yuan et al., 2017). Our study indicated that *Npas2* KO mutation increased fibroblast proliferation (Fig. 2B), which may have confounded the cell migration assay. When the time-lapse microscopy was evaluated (Video: https://players.brightcove.net/656326989001/default_default/index.html?videoId=6013197672001), no proliferating cells were observed within the scratch area for all genotypes, suggesting that the effect of *Npas2* on cell proliferation and migration occurs through mechanisms other than cell proliferation.

Previously, we reported that titanium-based biomaterials increased the *Npas2* expression of bone marrow mesenchymal stromal cells (BMSC) concomitantly with an elevated expression of cartilage collagens types II, IX, and X, suggesting that *Npas2* might mediate biomaterial-induced BMSC differentiation (Mengatto et al., 2011). Thus, our first step of mechanistic dissection was to examine skin fibroblast differentiation through dermal-related collagens. Skin dermal collagen ECM is primarily composed of fibril-forming type I and type III collagens, which form thick collagen fibers (Gordon and Hahn, 2010). FACIT collagen types XII and XIV have been found in developing skin (Castagnola et al., 1992; Oh et al., 1993; Berthod et al., 1997). Type XII and XIV colla-gens are postulated to decorate

the surface of collagen fibers and regulate the physiological ECM organization with tissue-specific functions. By contrast, wound fibroblasts abundantly synthesize collagen ECM with different properties in the GT. Our study revealed a striking upregulation of FACIT collagen types XII and XIV by *Npas2* KO fibroblasts (Fig. 4A). The *in vitro* collagen fiber formation depicted by picrosirius red staining showed thick collagen fibers in the cultures of *Npas2*+/− and *Npas2*−/− fibroblasts (Fig. 4B,C). The robustly increased FACIT expression might contribute to the re-organization of dermis-like collagen fibers in the skin wound. In fact, *Npas2*−/− mice demonstrated an increased WCA containing mature dermis-like collagen structure (Fig. 5A). Furthermore, the GT of *Npas2*−/− mice showed thicker collagen fibers, in part, resembling the dermis-like collagen fiber structure. Taken together, we propose that fibroblasts with decreased *Npas2* expression may differentiate to dermal fibroblasts, not myofibroblasts or GT fibroblasts, and Npas2-suppressed fibroblasts might induce their ability to better reconstruct, if not partially regenerate, the dermal collagen architecture.

CONCLUSION

Our study demonstrated that *Npas2* suppression in peripheral skin fibroblasts modified cell behaviors and was depicted by accelerated cell proliferation, cell migration, and cell contraction forces in vitro. Moreover, Npas2 suppression resulted in increased dermis FACIT collagen synthesis and the formation of thick collagen fibers. These fibroblastic phenotypes appeared to have contributed to better skin wound healing and the potential reconstruction of dermis collagen architecture. Within the scope of this article, the mechanism of circadian clock molecules, such as Npas2, in dermal wound healing may facilitate skin-specific cell differentiation. From these results, we propose that Npas2 may be an attractive therapeutic target for improving skin wound healing.

Supplementary Material

Refer to Web version on PubMed Central for supplementary material.

ACKNOWLEDeGEMENTS

We thank Dr. Christopher S. Colwell and Dr. Yu Tahara, Department of Psychiatry & Biobehavioral Science, David Geffen, School of Medicine at UCLA, Los Angeles, CA for data interpretation of clock gene expression. We also thank Dr. Ivan Pushkarsky, Department of Bioengineering, UCLA Henry Samueli School of Engineering and Applied Science, Los Angeles, CA for technical assistance of the single-cell contraction assay. This study was supported, in part, by a UCLA Faculty Seed Grant (IN) and conducted in a facility constructed with support from the Research Facilities Improvement Program Grant Number C06 RR014529 from the National Center for Research Resources, National Institutes of Health (NCRR/NIH).

Grant sponsor: NIH/NCRR; Grant number: C06 RR014529; Grant sponsor: UCLA School of Dentistry; Grant number: Faculty Seed Grant.

LITERATURE CITED

Akhtar RA, Reddy AB, Maywood ES, Clayton JD, King VM, Smith AG, Gant TW, Hastings MH, Kyriacou CP. 2002 Circadian cycling of the mouse liver transcriptome, as revealed by cDNA microarray, is driven by the suprachiasmatic nucleus. Curr Biol 12: 540–550. [PubMed: 11937022]

Berthod F, Germain L, Guignard R, Lethias C, Garrone R, Damour O, van der Rest M, Auger FA. 1997 Differential expression of collagens XII and XIV in human skin and in reconstructed skin. J Invest Dermatol 108:737–742. [PubMed: 9129225]

Bertolucci C, Cavallari N, Colognesi I, Aguzzi J, Chen Z, Caruso P, Foá A, Tosini G, Bernardi F, Pinotti M. 2008 Evidence for an overlapping role of CLOCK and NPAS2 transcription factors in liver circadian oscillators. Mol Cell Biol 28:3070–3075. [PubMed: 18316400]

Brown RA, Sethi KK, Gwanmesia I, Raemdonck D, Eastwood M, Mudera V. 2002 Enhanced fibroblast contraction of 3D collagen lattices and integrin expression by TGF-beta1 and -beta3: mechanoregulatory growth factors? Exp Cell Res 274:310–322. [PubMed: 11900491]

Bunger M, Wilsbacher LD, Moran SM, Clendenin C, Radcliffe LA, Hogenesch JB, Simon MC, Takahashi JS, Bradfield CA. 2000 Mop3 is an essential component of the master circadian pacemaker in mammals. Cell 103:1009–1017. [PubMed: 11163178]

Castagnola P, Tavella S, Gerecke DR, Dublet B, Gordon MK, Seyer J, Cancedda R, van der Rest M, Olsen BR. 1992 Tissue-specific expression of type XIV collagen-- a member of the FACIT class of collagens. Eur J Cell Biol 59:340–347. [PubMed: 1493799]

Chen JC, Lin BB, Hu HW, Lin C, Jin WY, Zhang FB, Zhu YA, Lu CJ, Wei XJ, Chen RJ. 2014 NGF accelerates cutaneous wound healing by promoting the migration of dermal fibroblasts via the PI3K/Akt-Rac1-JNK and ERK pathways. Biomed Res Int 2014:547187.

Conroy KP, Kitto LJ, Henderson NC. 2016 aV integrins: key regulators of tissue fibrosis. Cell Tissue Res 365:511–519. [PubMed: 27139180]

Ehrlich HP, Rajaratnam JB. 1990 Cell locomotion forces versus cell contraction forces for collagen lattice contraction: an in vitro model of wound contraction. Tissue Cell 22:407–417. [PubMed: 2260082]

Fiore VF, Wong SS, Tran C, Tan C, Xu W, Sulchek T, White ES, Hagood JS, Barker TH. 2018 Avb3 integrin drives fibroblast contraction and strain stiffening of soft provisional matrix during progressive fibrosis. JCI Insight 3(20):e97597.

Franzoni A, Markova-Car E, Dević-Pavlić S, Jurišić D, Puppin C, Mio C, De Luca M, Petruz G, Damante G, Pavelić SK. 2017 A polymorphic GGC repeat in the NPAS2 gene and its association with melanoma. Exp Biol Med 242:1553–1558.

Gilles-Gonzalez MA, Gonzalez G. 2004 Signal transduction by heme-containing PAS-domain proteins. J Appl Physiol 96: 774–783. [PubMed: 14715687]

Glass D, Viñuela A, Davies MN, Ramasamy A, Parts L, Knowles D, Brown AA, Hedman AK, Small KS, Buil A, et al. 2013 Gene expression changes with age in skin, adipose tissue, blood and brain. Genome Biol 14:R75. [PubMed: 23889843]

Gordon MK, Hahn RA. 2010 Collagens. Cell Tissue Res 339:247–257. [PubMed: 19693541]

Grassel S, Bauer RJ. 2013 Collagen XVI in health and disease. Matrix Biol 32:64–73. [PubMed: 23149016]

Grinnell F 1994 Fibroblasts, myofibroblasts, and wound contraction. J Cell Biol 124:401–404. [PubMed: 8106541]

Haque R, Ali FG, Biscoglia R, Abey J, Weller J, Klein D, Iuvone PM. 2010 CLOCK and NPAS2 have overlapping roles in the circadian oscillation of arylalkylamine N-acetyltransferase mRNA in chicken cone photoreceptors. J Neurochem 113:1296–1306. [PubMed: 20345751]

Hoyle NP, Seinkmane E, Putker M, Feeney KA, Krogager TP, Chesham JE, Bray LK, Thomas JM, Dunn K, Blaikley J, et al. 2017 Circadian actin dynamics drive rhythmic fibroblast mobilization during wound healing. Sci Transl Med 9:eaal2774.

Kendall RT, Feghali-Bostwick CA. 2014 Fibroblasts in fibrosis: novel roles and mediators. Front Pharmacol 5:123. [PubMed: 24904424]

Klein G, Kibbler C, Schermutzki F, Brown J, Muller CA, Timpl R. 1998 Cell binding properties of collagen type XIV for human hematopoietic cells. Matrix Biol 16(6):307–317. [PubMed: 9503364]

Kowalska E, Ripperger JA, Hoegger DC, Bruegger P, Buch T, Birchler T, Mueller A, Albrecht U, Contaldo C, Brown SA. 2013 NONO couples the circadian clock to the cell cycle. Proc Natl Acad Sci USA 110:1592–1599. [PubMed: 23267082]

Koziol-White CJ, Yoo EJ, Cao G, Zhang J, Papanikolaou E, Pushkarsky I, Andrews A, Himes BE, Damoiseaux RD, Liggett SB, et al. 2016 Inhibition of PI3K promotes dilation of human small airways in a rho kinase-dependent manner. Br J Pharmacol 173: 2726–2738. [PubMed: 27352269]

Landgraf D, Wang LL, Diemer T, Welsh DK. 2016 NPAS2 Compensates for Loss of CLOCK in Peripheral Circadian Oscillators. PLoS Genet 12:e1005882.

Li G, Li YY, Sun JE, Lin WH, Zhou RX. 2016 ILK-PI3K/AKT pathway participates in cutaneous wound contraction by regulating fibroblast migration and differentiation to myofibroblast. Lab Invest 96:741–751. [PubMed: 27111285]

Liu Y, Ko JA, Yanai R, Kimura K, Chikama T, Sagara T, Nishida T. 2008 Induction by latanoprost of collagen gel contraction mediated by human tenon fibroblasts: role of intracellular signaling molecules. Invest Ophthalmol Vis Sci 49:1429–1436. [PubMed: 18385060]

Mengatto CM, Mussano F, Honda Y, Colwell CS, Nishimura I. 2011 Circadian rhythm and cartilage extracellular matrix genes in ossoeintegration: a genome-wide screening of implant failure by vitamin D deficiency. PLoS One 6(1):e15848.

McNamara P, Seo SB, Rudic RD, Sehgal A, Chakravarti D, FitzGerald GA. 2001 Regulation of CLOCK and MOP4 by nuclear hormone receptors in the vasculature: a humoral mechanism to reset a peripheral clock. Cell 105:877–889. [PubMed: 11439184]

Miller BH, Olson SL, Turek FW, Levine JE, Horton TH, Takahashi JS. 2004 Circadian clock mutation disrupts estrous cyclicity and maintenance of pregnancy. Curr Biol 14:1367–1373. [PubMed: 15296754]

Mulero-Navarro S, Pozo-Guisado E, Perez-Mancera PA, Alvarez- Barrientos A, Catalina-Fernandez I, Hernandez-Nieto E, Saenz-Santamaria J, Martinez N, Rojas JM, Sanchez-Garcia I, et al. Immortalized mouse mammary fibroblasts lacking dioxin receptor have impaired tumorigenicity in a subcutaneous mouse xenograft model. J Biol Chem 280(31):28731–28741.

Nagoshi E, Saini C, Bauer C, Laroche T, NaefF Schibler U., 2004 Circadian gene expression in individual fibroblasts: cell-autonomous and self-sustained oscillators pass time to daughter cells. Cell 119: 693–705. [PubMed: 15550250]

Nishiyama T, McDonough AM, Bruns RR, Burgeson RE. 1994 Type XII and XIV collagens mediate interactions between banded collagen fibers in vitro and may modulate extracellular matrix deformability. J Biol Chem 269(45):28193–28199. [PubMed: 7961756]

Ngo P, Ramalingam P, Phillips JA, Furuta GT. 2006 Collagen gel contraction assay. Methods Mol Biol 341:103–109. [PubMed: 16799192]

Oh SP, Griffith CM, Hay ED, Olsen BR. 1993 Tissue-specific expression of type XII collagen during mouse embryonic development. Dev Dyn 196(1):37–46. [PubMed: 8334298]

Oishi K, Atsumi G, Sugiyama S, Kodomari I, Kasamatsu M, Machida K, Ishida N. 2006 Disrupted fat absorption attenuates obesity induced by a high-fat diet in Clock mutant mice. FEBS Lett 580:127–130. [PubMed: 16343493]

O'Neil D, Mendez-Figueroa H, Mistretta TA, Su C, Lane RH, Aagaard KM. 2013 Dysregulation of Npas2 leads to altered metabolic pathways in a murine knockout model. Mol Genet Metab 110:378–387. [PubMed: 24067359]

Pushkarsky I, Tseng P, Black D, France B, Warfe L, Koziol-White CJ, WFJr J, Trinh RK, Lin J, Scumpia PO, et al. 2018 Elastomeric sensor surfaces for high-throughput single-cell force cytometry. Nat Biomed Eng 2:124–137. [PubMed: 31015629]

Schiro JA, Chan BM, Roswit WT, Kassner PD, Pentland AP, Hemler ME, Eisen AZ, Kupper TS. 1991 Integrin alpha 2 beta 1 (VLA-2) mediates reorganization and contraction of collagen matrices by human cells. Cell 67:403–410. [PubMed: 1913826]

Sipahi M, Zengin K, Tanik S, Arslan E, Qubukgu A. 2014 Effects of circadian rhythm disorders on wound healing and strength of bowel anastomosis in rats. Wounds 26:317–322. [PubMed: 25856166]

Style RW, Boltyanskiy R, German GK, Hyland C, MacMinn CW, Mertz AF, Wilen LA, Xu Y, Dufresne ER. 2014 Traction force microscopy in physics and biology. Soft Matter 10:4047–4455. [PubMed: 24740485]

Turek FW, Joshu C, Kohsaka A, Lin E, Ivanova G, McDearmon E, Laposky A, Losee-Olson S, Easton A, Jensen DR, et al. 2005 Obesity and metabolic syndrome in circadian Clock mutant mice. Science 308:1043–1045. [PubMed: 15845877]

Vitaterna MH, King DP, Chang AM, Kornhauser JM, Lowrey PL, McDonald JD, Dove WF, Pinto LH, Turek FW, Takahashi JS. 1994 Mutagenesis and mapping of a mouse gene, Clock, essential for circadian behavior. Science 64:719–725.

Wijnen H, Young MW. 2006 Interplay of circadian clocks and metabolic rhythms. Annu Rev Genet 40:409–448. [PubMed: 17094740]

Xue X, Liu F, Han Y, Li P, Yuan B, Wang X, Chen Y, Kuang Y, Zhi Q, Zhao H. 2014 Silencing NPAS2 promotes cell growth and invasion in DLD-1 cells and correlated with poor prognosis of colorectal cancer. Biochem Biophys Res Commun 450:1058–1062. [PubMed: 24978311]

Yamamoto T, Nakahata Y, Soma H, Akashi M, Mamine T, Takumi T. 2004 Transcriptional oscillation of canonical clock genes in mouse peripheral tissues. BMC Mol Biol 5:18. [PubMed: 15473909]

Yuan P, Li J, Zhou F, Huang Q, Zhang J, Guo X, Lyu Z, Zhang H, Xing J. 2017 NPAS2 promotes cell survival of hepatocellular carcinoma by transactivating CDC25A. Cell Death Dis 8:e2704. [PubMed: 28333141]

Zhou YD, Barnard M, Tian H, Li X, Ring HZ, Francke U, Shelton J, Richardson J, Russell DW, McKnight SL. 1997 Molecular characterization of two mammalian bHLH-PAS domain proteins selectively expressed in the central nervous system. Proc Natl Acad Sci USA 94:713–718. [PubMed: 9012850]

Zhu Y, Leaderer D, Guss C, Brown HN, Zhang Y, Boyle P, Stevens RG, Hoffman A, Qin Q, Han X, et al. 2007 Ala394Thr polymorphism in the clock gene NPAS2: a circadian modifier for the risk of non- Hodgkin's lymphoma. Int J Cancer 120:432–435. [PubMed: 17096334]

Zhu Y, Stevens RG, Leaderer D, Hoffman A, Holford T, Zhang Y, Brown HN, Zheng T. 2008 Non-synonymous polymorphisms in the circadian gene NPAS2 and breast cancer risk. Breast Cancer Res Treat 107:421–425. [PubMed: 17453337]

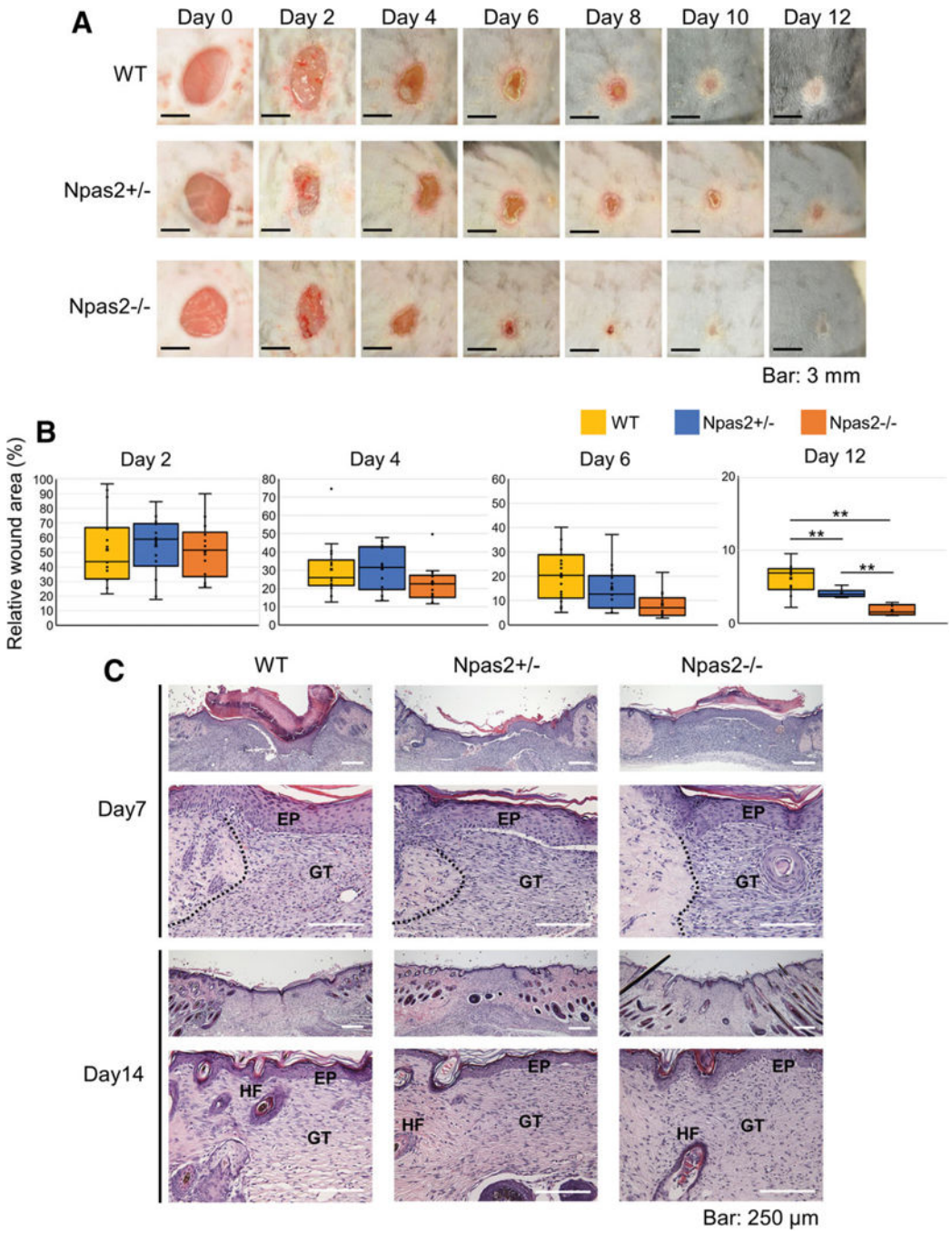

Fig. 1.

Full-thickness skin punch wound healing. (**A**) A standardized photograph of the skin wound was obtained from 0 to 12 days after surgery, depicting the progressive wound closure and contraction. (**B**) The relative wound area was calculated at 2, 4, 6, and 12 days. *Npas2* KO mice showed a significantly smaller wound area than that of WT mice at day 12 (** $P <$ 0.01). (**C**) Histological observation of wounds at Day 7 showed the formation of granulation tissue (GT) and the restoration of epithelial integrity (EP); however, the wound margin

(dotted line) was clearly observed. At Day 14, the wound margin highlighted by hair follicles (HFs) was less clear and approached toward the granulation tissue (GT).

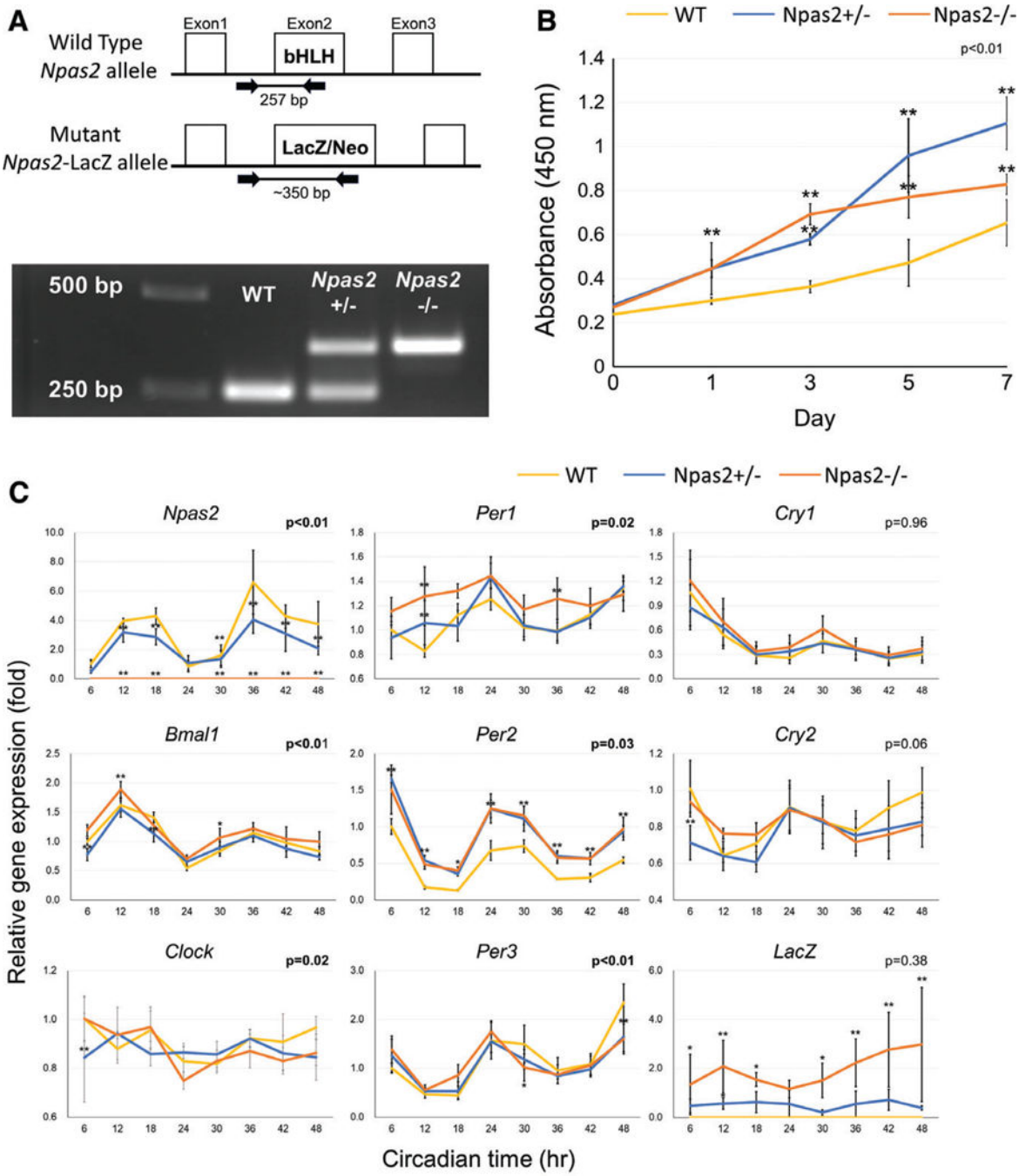

Fig. 2.

Characterization of WT, *Npas2+/−,* and *Npas2−/−* skin fibroblasts. (**A**) The genotype of each fibroblast batch was determined by genomic DNA PCR. The WT *Npas2* allele generated a 250 bp PCR product, whereas the mutant allele generated a 350 bp PCR product. (**B**) The WST-1 assay demonstrated the increased cell proliferation rate in *Npas2* KO fibroblasts (** $P < 0.01$, significant difference compared with WT at the time points *via* the Tukey analysis). (**C**) The expression of core clock genes and the *LacZ* reporter gene was determined by RT-PCR every 6 for 48 hr (*P* value in the figure: two-way ANOVA for the interaction between

the time and genotype factors. *$P < 0.05$, **$P < 0.01$, significant difference compared with WT at the time points *via* the Tukey analysis) (C).

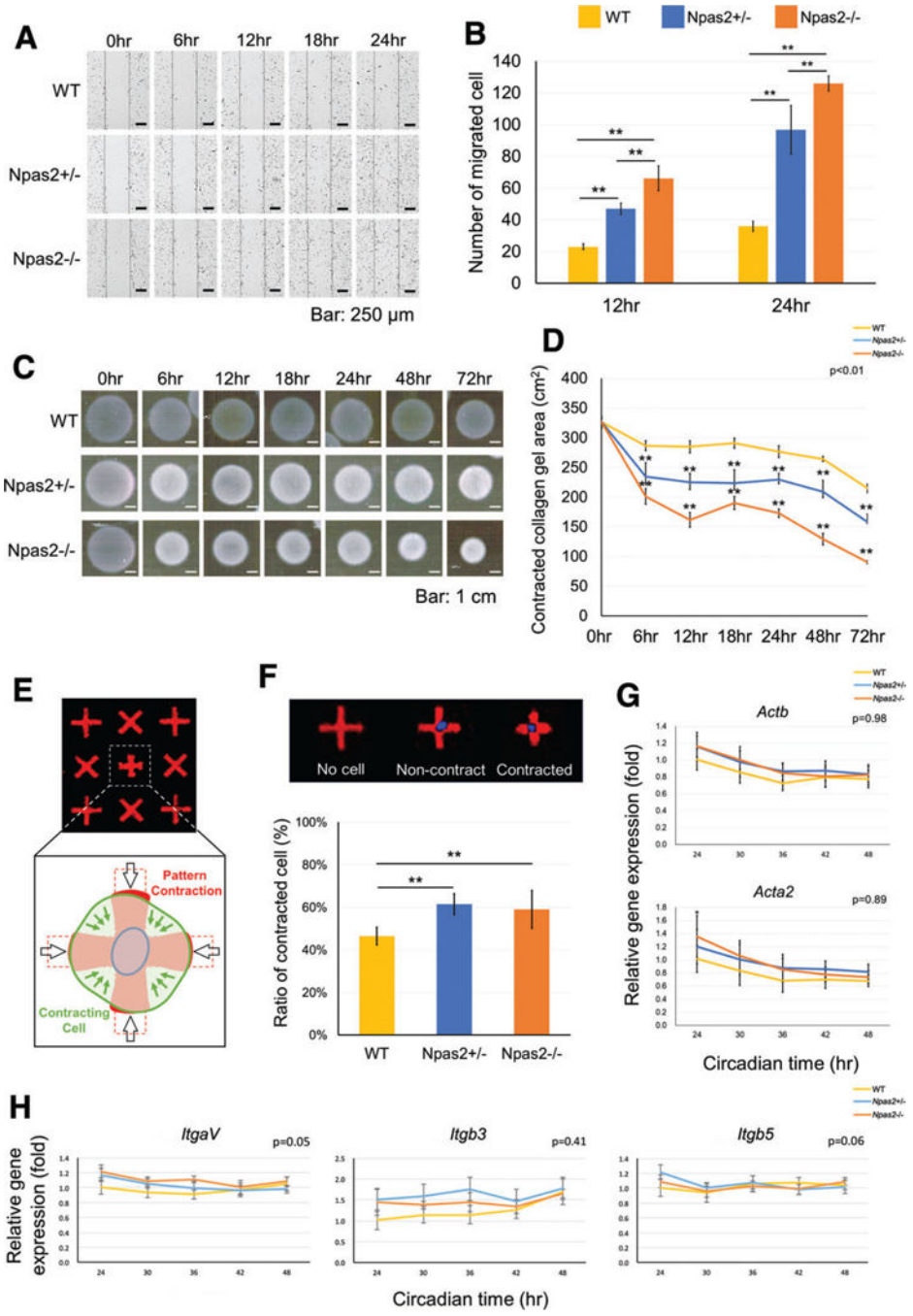

Fig. 3.

In vitro wound healing experiment using WT, *Npas2+/−* and *Npas2−/−* fibroblasts. (**A**) Images of time-lapse micrographs captured the progressive scratch wound healing assay. The number of migrated cells within the scratched area was significantly larger in the *Npas2* KO groups at 6 hr and 12 hr (***P* < 0.01). (**C**) Standardized images of floating collagen gel depicted an increased collagen gel contraction in the *Npas2* KO fibroblast groups. (**D**) The area of collagen gels decreased over time. The gel contraction speed was faster in *Npas2* KO fibroblasts (***P* < 0.01, significant difference shown only compared with WT). (**E**)

Schematic presentation of the FLECS-based single-cell contraction. (**F**) The ratio of contracted cells was increased in *Npas2* KO fibroblasts. (**G**) *Npas2* KO mutation did not affect the gene expression of β-actin (Actb) and α-SMA (*Acta2*) in dermal fibroblasts. (**H**) The steady state gene expression level of integrin subunits αV *(ItgaV),* β3 *(Itgb3),* and β5 *(Itgb5)* in dermal fibroblasts was not affected by *Npas2* KO mutation.

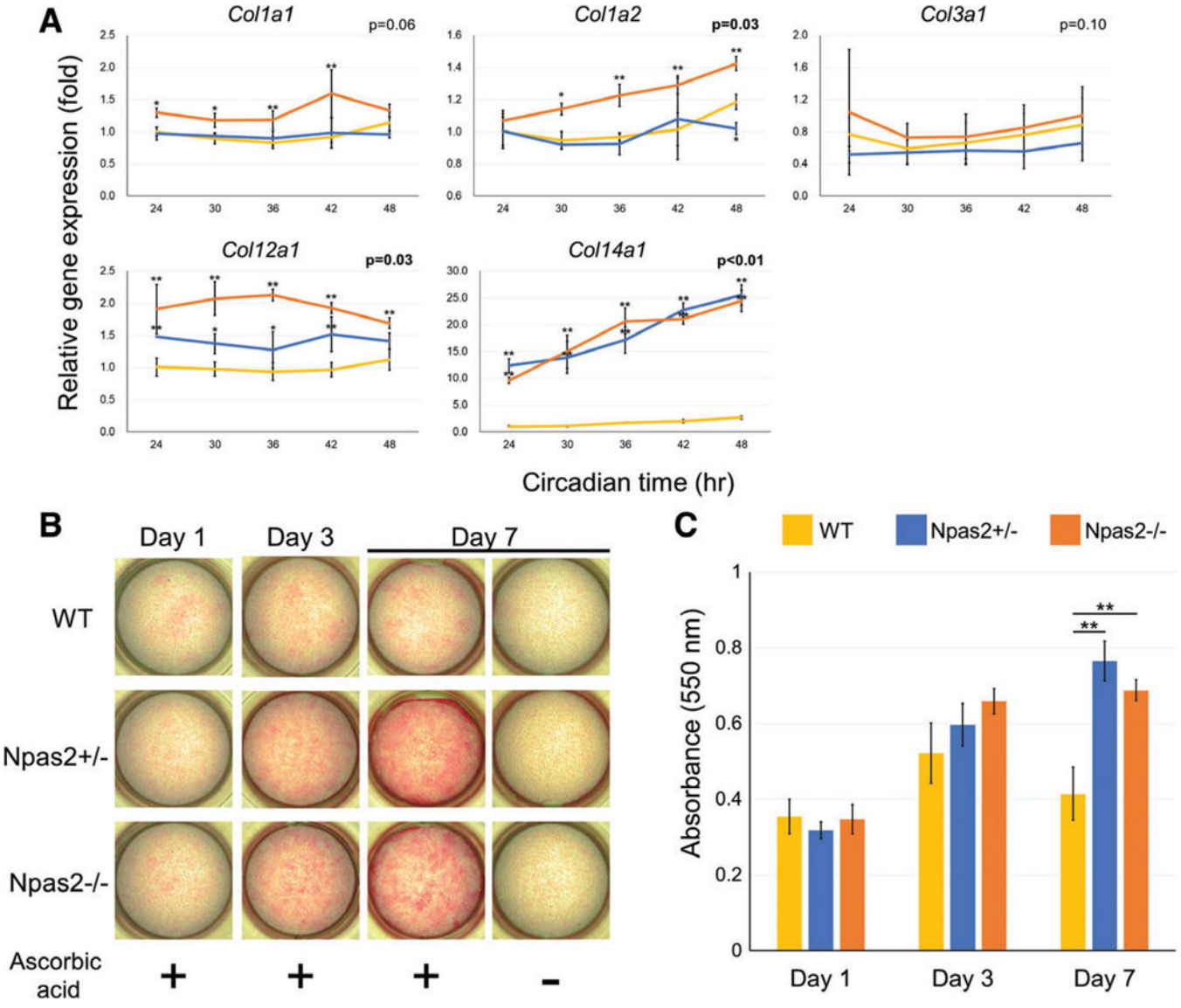

Fig. 4.

Collagen synthesis by WT, *Npas2+/−* and *Npas2−/−* fibroblasts *in vitro.* (**A**) Gene expression of collagen type I (*Collal* and *Colla2),* type III *(Col3a1),* type XII *(Coll2a1),* and type XIV *(Coll4a1)* (**$P < 0.01$, *$P < 0.05$, significant difference shown only compared with WT). FACIT collagen type XII and type XIV showed significantly increased steady-state mRNA levels in *Npas2+/−* and *Npas2−/−* fibroblasts. (**B**) Images for cultured fibroblasts with picrosirius red staining highlighted the synthesis of collagen fibers. (C) The *in vitro* collagen fiber deposition was measured by picrosirius red staining (**$P < 0.01$ by one-way ANOVA with *post hoc* Holm test).

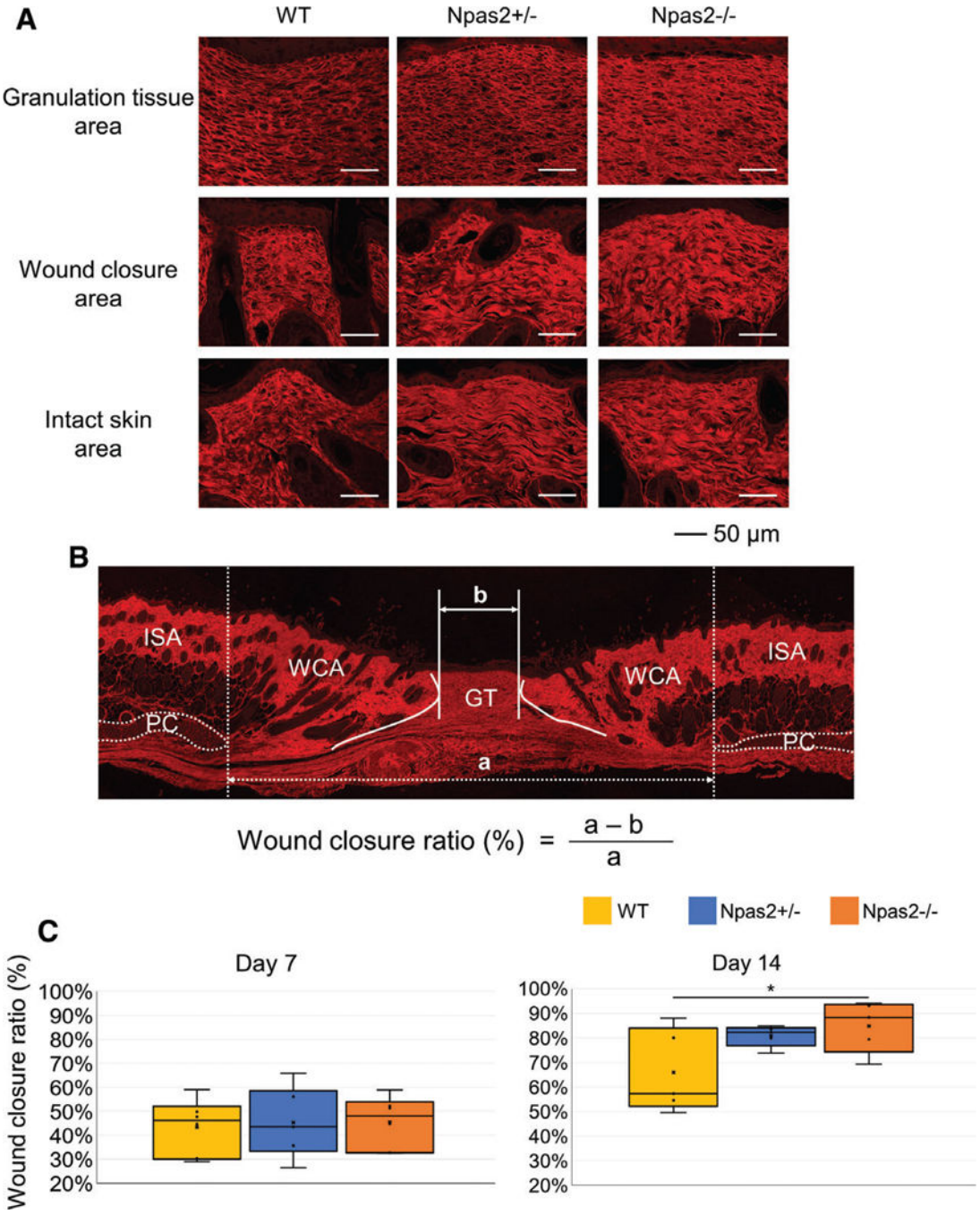

Fig. 5.

Evaluation of collagen fiber structure in the wound healing area. (**A**) Confocal laser scanning microscopy depicted the collagen fiber architecture stained with picrosirius red at 14 days after surgery. (**B**) Measurement of the wound closure ratio using the wound closure area (WCA) calculated as the width of the ISA (a) between *panniculus carnosus* (PC) subtracted by the granulation tissue area (GT: b), which was normalized by ISA. (**C**) The

wound closure ratio was greater in *Npas2*+/− and *Npas2*−/− mice at Day 14, albeit statistical significance was achieved only between the WT and *Npas2*−/− groups.